ELSEVIER

Contents lists available at ScienceDirect

## Bioresource Technology

journal homepage: www.elsevier.com/locate/biortech





# From waste to adsorbent: Properties of CO<sub>2</sub>-activated biochars from pistachio hulls and walnut shells for advanced water remediation

Federica Menegazzo <sup>a,\*</sup>, Rony Snyders <sup>b,c</sup>, Carla Bittencourt <sup>b</sup>, Melissa Del Carmen Bello Pinzon <sup>a</sup>, Elena Ghedini <sup>a,d</sup>, Michela Signoretto <sup>a</sup>

- <sup>a</sup> CATMAT Lab, Department of Molecular Sciences and Nanosystems, Ca' Foscari University of Venice and INSTM RUVe, via Torino 155, 30172 Venezia Mestre, Italy <sup>b</sup> Chimie des Interactions Plasma-Surface (ChIPS), CIRMAP, Research Institute for Materials Science and Engineering, University of Mons, 23 Place du Parc, B-7000 Mons. Belgium
- <sup>c</sup> Materia Nova Research Center, 3 avenue Copernic, 7000 Mons, Belgium
- d Chemistry Department, Università degli Studi di Bari Aldo Moro, 70125 Bari, Italy

#### HIGHLIGHTS

- CO<sub>2</sub> –activated biochars from agriwaste were synthesized.
   Properties were modulated by pyrolysis
- and acid washing.

   High atrazine removal, comparable to
- commercial carbon.

   Acid washing had no effect on pesticide
- adsorption.
- Waste-derived biochars for eco-friendly water remediation.

## G R A P H I C A L A B S T R A C T



## ARTICLE INFO

Keywords:
Pyrolysis
Water treatment
Pesticide
Atrazine
Sorption

## ABSTRACT

This study investigates the properties of  $CO_2$ -activated biochars derived from second-generation agricultural waste, specifically pistachio hulls and walnut shells. The biochars were prepared using varying pyrolysis temperatures of 500 °C and 750 °C, followed by physical activation with  $CO_2$  at 850 °C and, in some cases, acid washing. A range of characterization techniques were used to assess the effects of biomass type, pyrolysis temperature, and acid-washing on the biochars' properties. This comprehensive analysis provided insights into the surface chemistry and structural characteristics of biochars. The results demonstrate the significant versatility of pyrolysis in modulating the properties of the resultant biochars. Sorption experiments with atrazine showed high removal efficiencies (94–95 %), comparable to commercial active carbon. Notably, the acid washing treatment did not affect pesticide sorption. These findings indicate the potential of using waste-derived biochars as high-performance sorbents for sustainable water remediation and circular economy initiatives.

E-mail address: federica.menegazzo@unive.it (F. Menegazzo).

 $<sup>^{\</sup>ast}$  Corresponding author.

#### 1. Introduction

Transforming agricultural residues into high-value biochar is an ecofriendly method for waste management and resource re-utilization, supporting sustainability goals and circular economy. Crop waste is often generated in large quantities as by-products of food production and processing. Traditionally, these residues are left to decompose, incinerate, or used in low-value applications, contributing to greenhouse gas emissions, soil acidification, eutrophication, and atmospheric contamination. By upcycling these residues into biochar by pyrolysis processes (Lu & Gu, 2022), it can harness their potential as alternative renewable energy sources, soil amendments, and sorbents for water purification (Singh & Verma, 2024; Tan et al., 2015). Upcycling promotes the efficient use of available resources, allowing valorization of waste that would otherwise have little to no market value, and minimizing the need for new raw materials. This could create new revenue streams and business opportunities, enhancing the overall economic viability of agricultural industries, while promoting and supporting the transition from a linear to a circular economy (Huang et al., 2021). Pyrolysis is one of the most used thermo-chemical processes for biomass degradation involving the thermolysis of organic materials at much lower temperatures than gasification and combustion (Wang et al., 2017). Pyrolysis conditions strongly influence the distribution and properties of the final products (Handiso et al., 2024; Rambhatla et al., 2025). The choice of feedstock is also a critical factor, influencing not only the yield but also the physical and chemical properties of the resulting biochar. The large-scale cultivation of pistachios and walnuts generates a significant quantity of waste, such as their shells, which often lack high value uses and are thus ideal candidates for upcycling into biochar. The annual global production is over 3 million tons of walnuts and 1.1 million tons of pistachios, with a continuous demand increase. Utilizing locally available agricultural by-products can also reduce transportation costs and environmental impact, further enhancing the overall sustainability of the process. For walnuts, the shell represents 30 to 40 % of the total walnut weight (Halysh et al., 2018; Korkut, 2011), while for pistachios, the shell typically comprises about 50 % of the total nut weight (Čolnik et al., 2024; Hosseinzaei et al., 2022; Pączkowski & Gawdzik, 2024). After the pyrolysis process, the biochar surface area is usually low, limiting its sorption capacity. Various modification techniques can be applied to improve its performance, such as physical activation or chemical ones using acids (H<sub>2</sub>PO<sub>4</sub>, H<sub>2</sub>SO<sub>4</sub>, HNO<sub>3</sub>), bases (NaOH, KOH), or salts (K<sub>2</sub>CO<sub>3</sub>, ZnCl<sub>2</sub>) (Huang et al., 2021). Other novel activations have been used, like microwave radiation, plasma modification, impregnation with metal oxides. Physical activation typically involves steam, H2O2, O2, NH3, or CO2 treatment. Activation with CO2 (Kim et al., 2019) gives an overall benefit by reducing greenhouse gas emissions at a low cost while reducing the usage of chemicals and increasing the formation of the microporous structure, surface area, and oxygen-containing functional groups. Moreover, acid washing (Gao et al., 2021) is a common post-pyrolysis treatment to remove inorganic impurities, ash content, and unblocking pores, thereby modifying the surface characteristics of the biochar. Biochar has garnered increasing attention in water treatment applications (Kokab et al., 2021). Atrazine (6-Chloro-N2-ethyl-N4- (propan-2yl)-1,3,5-triazine-2,4-diamine, C<sub>8</sub>H<sub>14</sub>ClN<sub>5</sub>) or ATZ, one of the most extensively used herbicides in the world, is a notorious contaminant due to its persistence in aquatic environments and potential health impacts, including endocrine disruption and cancer risks (Deng et al., 2024; Khoshnood, 2024; Singh et al., 2018; Song et al., 2014). Despite regulatory restrictions in many regions, ATZ continues to be detected in surface water and groundwater at concentrations exceeding permissible limits. In fact, it is characterized by being highly persistent in soil and water, due to its long half-life, pKa (1.7), and water solubility (33 mg/L 25 °C). Raising concerns about its impact underscores the importance of effective removal methods to prevent adverse health outcomes in humans and wildlife. Many countries have established maximum

allowable concentrations for drinking water, typically ranging from 0.1 to 3  $\mu$ g/L. The need to meet these stringent standards drives the demand for efficient water treatment technologies capable of reducing levels to safe limits. Conventional water treatment methods are often insufficient for removing small traces of micropollutants like pesticides, pharmaceutical traces, heavy metals, and other "emerging pollutants", leading to the research of alternative technologies (Tillvitz do Nascimento et al., 2022). Biochar offers several advantages over traditional sorbents used in water treatment, including cost-effectiveness, environmental benefits, and adaptability (Zhi et al., 2023). While active carbon is widely used for its high sorption capacity (Dong et al., 2024), its production is energy intensive. It has higher overall costs, considering operation, maintenance, transportation, and regeneration costs. Biochar's versatility and lower cost make it an attractive alternative, especially for applications where high performance is required at a lower cost (Wang et al., 2020). The production cost of biochar varies widely, depending on the type of feedstock and pyrolysis conditions, but can be significantly lower than that of activated carbon. Indeed, biochar production can be a less energy-intensive process, both in terms of production and management, and it uses low-cost or valueless agricultural waste. Furthermore, using feedstocks such as agricultural waste also reduces transportation costs. (Zhang, et al., 2022). Despite its promising potential, biochar application in water treatment faces several challenges, such as variability in feedstock materials and production processes can result in inconsistencies in biochar properties. Standardizing production methods, to ensure quality control, is essential for ensuring reliable performance and real application outcomes. The primary goal of this work is to produce and characterize activated biochars derived from agricultural residues, demonstrating the possibility of modulating their final properties. Walnut (WS) and pistachio shells (PS) were selected as the feedstocks, second-generation biomass supporting the principles of a circular economy and the concept of upcycling. The biochars were produced through slow pyrolysis of the biomasses at two different temperatures, physically activated with CO2. The activated biochars were employed as a sorbent for water purification, focusing on the removal of ATZ. The sorption capacities of the biochars were evaluated and compared with those of a commercial active carbon. Additionally, the study compares the sorption capabilities of acid-washed and nonwashed biochars to assess the impact of post-production treatments on their effectiveness.

## 2. Materials and methods

## 2.1. Materials

The reagents used in this work were:

Atrazine (>99,9% analytical grade, Sigma-Aldrich); Hydrochloric acid (Sigma-Aldrich, puriss. p.a., ACS reagent, fuming,  $\geq$ 37 %); A commercial active carbon supplied by Acque Veronesi S.P.A. PS and WS were bought in local markets in Venice (Italy).

## 2.2. Activated biochars synthesis

After consumption, PS and WS were grounded, sieved (1.2—2.8 mm), and dried at 110  $^{\circ}\text{C}$  in an oven for 24 h. The laboratory-scale prototype pyrolysis reactor (Carbolite custom model EVT 12/450B) consists of a horizontal furnace with a quartz tube reactor (Longo et al., 2022). The pyrolysis process (for approximately 30–40 g of biomass) was conducted under  $N_2$  flow (100 mL/min). A constant heating rate was set at 10  $^{\circ}\text{C}/\text{min}$  for and a resident time of 60 min The pyrolysis temperature was set at 500 or 750  $^{\circ}\text{C}$ . Post-pyrolysis, the biochar was subjected to a physical activation process, using CO<sub>2</sub> flow (100 mL/min) at 850  $^{\circ}\text{C}$  for 90 min (Longo et al., 2023). Some biochars were washed for 1 h under sonication with HCl (1 g of biochar with 20 mL HCl 1 M) and washed until pH = 7. The nomenclature of the biochars is reported in Table 1.

**Table 1** Biochars nomenclature.

Biomass	PyrolysisTemperature (°C)	Acid washing	Abbreviation
Walnut shell	750	no	WSB7(nw)
Walnut shell	750	yes	WSB7(w)
Walnut shell	500	no	WSB5(nw)
Walnut shell	500	yes	WSB5(w)
Pistachio shell	750	no	PIB7(nw)
Pistachio shell	750	yes	PIB7(w)
Pistachio shell	500	no	PIB5(nw)
Pistachio shell	500	yes	PIB5(w)

#### 2.3. Characterization

The Elemental analyses were conducted in duplicate using the UNICUBE elemental analyzer. The samples (2 mg) were previously thermally treated at 110 °C to remove residual moisture. FT-IR analyses were carried out using a PerkinElmer Spectrum One spectrometer and the traditional KBr pellet method. Spectra were recorded in the wavelength range of 400–4000 cm<sup>-1</sup> at a resolution of 4 cm<sup>-1</sup> and 32 scans. The results were analyzed using Spectrum One Software. TPD were performed using a lab-made equipment. The quartz reactor was charged with 50 mg of sample and heated to 1000 °C, with a heating rate of 10 °C/min under a helium flow (40 mL/min). Decomposition gases were recorded with a thermal conductivity detector (Gow-Mac 24-550 TCD instrument). The pH of the activated biochar sample was measured according to the Standard Test Method for pH of Activated Carbon ASTM D 3838. PZC was determined using the method of pH drift (Gatabi et al., 2015). N2 physisorption was analyzed using the MicroActive Tristar II Plus Micromeritics. The samples (100 mg) were degassed at 200 °C under vacuum for 2 h before measurement. The N2 apparent surface area (SBET) was calculated using the BET (Brunauer, Emmet, and Teller) equation within the (0.1 - 0.3) relative pressure  $(p/p_0)$  range. The total pore volume (V<sub>TOT</sub>) and pore size distribution were obtained by using the *t*-plot theory, at a relative pressure of 0.90 to the liquid volume of the adsorbate. SEM was carried out using a FE-SEM LEO 1525 ZEISS (Jena, DE), equipped with the SE2 and InLens detectors, with an acceleration potential voltage of 15 keV. Samples were deposited on the conductive carbon adhesive tape and metalized by sputtering with chromium (8 nm). XPS analyses were performed with a PHI Genesis instrument from Physical Electronics (Chanhassen, MN, USA), equipped with a monochromatic Al Ka X-ray source. To compensate for charge build-up during X-ray irradiation, a dual-mode charge compensation was used. The binding energy was calibrated based on the C 1 s peak at 284.6 eV.

## 2.4. Atrazine sorption test

The sorption capacity of the activated biochar for removing ATZ from water was determined through column adsorption tests. 2.5 g of sample, previously washed for 48 h in distilled water, was inserted into a 50 mL column. Then, 3.1 mL of a 150 ppm solution of atrazine in Milli-Q water was added on top, passed through the column, and analyzed. This process was repeated for ten cycles, each experiment was conducted in duplicate (Apolloni et al., 2025).

## 3. Results and discussion

While upcycling agricultural residues into biochar presents numerous benefits, several challenges must be addressed to realize its potential fully. First, not only can feedstock differences vary biochar properties, but environmental factors can also modulate the physicochemical characteristics produced from the same feedstock, leading to inconsistencies in performance. As for the production, it involves several critical steps that play a crucial role in determining the final properties of the biochar. Pyrolysis conditions, including temperature, residence time, and heating rate, influence biochar's physical structure, surface

chemistry, and sorption capacity (Janu et al., 2021; Muzyka et al., 2023). Moreover, acid washing is a common post-pyrolysis treatment used to enhance the properties of biochar. It involves treating the biochar with an acid solution to remove inorganic impurities, unblocking pores and modifying the surface characteristics of the biochar. The removal of inorganic impurities also minimizes potential interference with adsorption sites, thereby enhancing the biochar's overall sorption capacity and affinity for certain contaminants through mechanisms such as ion exchange or electrostatic attraction. This can lead to improved performance in water treatment applications where a high degree of contaminant removal is required (Hu et al., 2022; Uba Zango et al., 2024). Therefore, due to their versatility, it is crucial to investigate the properties of the final biochars to assess the most suitable treatment for the upcycling of a particular waste. At the same time, it is important to select which properties should primarily be checked when investigating a biochar. In this work, a series of analytical techniques were employed to determine physicochemical and structural characteristics, investigating the influence of different starting biomasses and synthesis conditions on the final properties of the biochars. The techniques included elemental analysis, Fourier Transform Infrared Spectroscopy (FTIR), programmed temperature desorption (TPD), pH and the point of zero charge (PZC), nitrogen physisorption, Scanning Electron Microscope (SEM), and X-ray photoelectron spectroscopy (XPS) to understand their properties comprehensively. The discussion aims to correlate the influence of the starting biomass feedstock and synthesis conditions, and how these factors influence the final properties of the materials. Moreover, it aims to define what techniques are more useful, less expensive, and could be used as a routine characterization when dealing with new active carbons. A comparative analysis was also conducted between the synthesized biochars and a commercial activated carbon used as a reference.

First, elemental analyses were used to determine the elemental composition of the biochars, allowing the quantification of carbon, hydrogen, nitrogen, and sulfur (Table 2). The three major key components in both biomasses are cellulose, hemicellulose, and lignin, distributed in the cell wall, and other minor non-structural elements. such as ash content, volatiles, extractives (fats, resin, pigments, etc.), and metals (Ca, K, Mg, Fe, Cu, etc.). Even though biomass chemical composition might differ slightly due to climatic conditions and cultivation geographic area, WS contain a larger content of lignin (35-55 %) and cellulose (25 - 35%) than hemicellulose (20 - 30%), as stated in the physicochemical characterization performed by Nair et al.(2023) with similar results reported by Fordos et al. (2023). PS contain a major quantity of cellulose (30-55 %) and hemicellulose (20-30 %) than lignin (10-30 %) (Saracoglu & Coruh, 2024). PIB and WSB biochars exhibit a high content of carbon in the range of 90 – 97 %, and after the acid-wash treatment, the carbon content even increases, with WSB7 acid-washed (w) being the highest (98 %). Commercial carbon is also rich in carbon content (87 %), even if lower than the synthesized biochars. On the contrary, biochars synthesized in this work have a very low amount of S with respect to the commercial sample. To collect information about the structure and composition of the biochar's surface and identify functional groups present, the FT-IR technique was used (Fig. 1a). The first signal that can be observed is a broad peak in the 3200–3600 cm<sup>-1</sup> range attributed to O-H stretching vibrations of hydroxyl groups, which can be related to the presence of moisture within the biochar's surface or

**Table 2** Elemental composition.

Sample	N [%]	C [%]	H [%]	S [%]
Commercial carbon	$0.44\pm0.02$	$87.12\pm0.03$	$0.70\pm0.01$	$0.51\pm0.01$
WSB7 (nw)	$0.31\pm0.02$	$91.31\pm0.03$	$0.91\pm0.01$	$0.14\pm0.01$
WSB7 (w)	$0.30\pm0.02$	$97.74 \pm 0.03$	$1.04\pm0.01$	$0.04\pm0.01$
PIB7 (nw)	$0.23\pm0.02$	$89.92\pm0.03$	$1.32\pm0.01$	$0.05\pm0.01$
PIB7 (w)	$0.24 \pm 0.02$	$93.50\pm0.03$	$0.70\pm0.01$	0

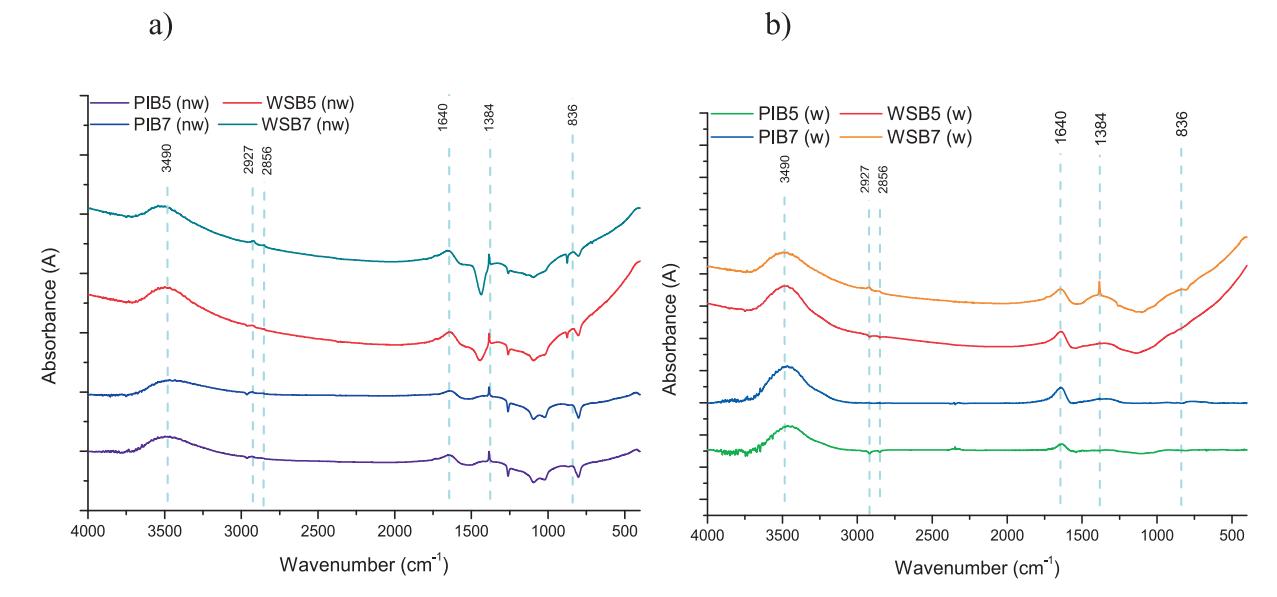


Fig. 1. FT-IR spectra of non-washed (section a) and acid-washed (section b) biochars.

hydroxyl groups of phenols, alcohol, or carboxyl. Two weak and lowintensity peaks at 2927 and 2856 cm<sup>-1</sup> can be attributed to the symmetrical and asymmetrical stretching vibrations of C-H bonds in aliphatic carbons (residues of lignin, cellulose, or organic compounds non-completely carbonized during activation). This indicates that the samples are almost completely carbonized after the CO<sub>2</sub>-activation process at high temperatures, eliminating most of the residual lignocellulosic content, or other organic compounds such as aliphatic bonds often seen in the stretching of -CH2 and -CH3 groups. A weak peak at 1640 cm<sup>-1</sup> can be interpreted as an overlap between C≡O stretching and C=C stretching vibrations, typically found in the range 1650-1750 and 1550–1650 cm<sup>-1</sup> respectively (Ozpinar et al., 2022). The former, C=O stretching vibrations indicate the presence of oxygen-containing groups such as carboxylic acids, ketones, aldehydes, quinones, or esters commonly present on the surface of activated biochar, most likely due to partial oxidation. The latter, C=C stretching vibrations, are characteristics of the aromatic rings formed during the carbonization process. In PIB biochars' spectra, this band is less prominent than in WSB, indicating a lower content of oxygen-containing functional groups. The narrow peak at 1384 cm<sup>-1</sup> can be attributed to C—H bending in aliphatic carbons, chains remaining after activation, indicating the presence of this type of functional group on the surface. No visible peak around 1260 cm<sup>-1</sup>, typically attributed to C—O stretching vibrations (1000-1300 cm<sup>-1</sup>), suggests the absence of carboxylic acids and alcohol functional groups in all samples. The CO2 activation can cause the reduction of some of these groups while potentially creating new functionalities. Finally, the peak at 836 cm<sup>-1</sup> can be attributed to the out-of-plane bending vibrations of C-H bonds typical of aromatic rings, (Fu et al., 2010). WSB spectrums show a relatively higher peak intensity than PIB spectra. The FTIR spectra of the biochars are very similar to the spectrum of the commercial carbon (see supplementary materials, Fig. S1). After acid-wash treatment (Fig. 1b), most signals disappear from both WSB and PIB biochars, indicating little to no presence of functional groups remaining in the surface structure. Only the broader band observed at 3490 cm<sup>-1</sup>, associated with the O-H stretching vibrations of hydroxyl groups, is more pronounced after the acid wash, in both biochars. The two low-intensity peaks at 2927 and 2856 cm<sup>-1</sup>, associated with C—H stretching vibrations, and the peak at  $1384~\text{cm}^{-1}$  are visible only in the WSB7 spectrum, suggesting a low aliphatic carbon content in the other activated biochars. A wide medium intensity peak at 1640 cm<sup>-1</sup>, more visible for walnut shell samples, was retained after acid-washing, reasonably indicating the presence of

aromatic rings formed during the carbonization process. The presence of the peak at 836 cm<sup>-1</sup>, supports the presence of aromatic rings or conjugated systems on these biochars after the acid-wash treatment. The comparison between walnut shell and pistachio shell biochar indicates that both feedstocks follow similar trends in response to pyrolysis temperature. However, walnut shell biochar tends to exhibit slightly stronger aromatic features at comparable temperatures. The differences can be primarily attributed to variations in their lignocellulosic content. Moreover, the acid-wash treatment significantly alters the biochar's surface chemistry, evidencing the absence of functional groups.

The TPD data for biochars allows us to further understand their surface chemistry and their thermal stability. TPD analysis is a widely utilized technique for detecting surface oxygen-containing functional groups on the surface of carbonaceous materials. Functional groups in the analysis undergo thermal decomposition into CO, CO<sub>2</sub>, and H<sub>2</sub>O at different temperatures depending on the thermal stability of the specific functional group being analyzed. Fig. 2 shows the TPD results before (a) and after (b) the acid-wash treatment. Non-washed WSB biochars present a similar profile. First, a low-intensity peak with a gradual increase in the 100—400 °C range, called the low-temperature region, can be attributed to H2O and CO2 desorption peaks of less stable carboxylic acids, anhydrides, or lactone functional groups. WSB7 exhibits a narrower and sharper peak around 150 °C, indicating a higher content of more stable surface oxygen groups compared to WSB5 Non-washed PIB samples present a gradual intensity increase but no pronounced peak in this region; this suggests that oxygen-containing groups in PS biochar are less abundant or less thermally stable compared to those in WSB, in agreement with what was found by FTIR. A sharp and narrow peak around 650 °C, attributed to CO desorption typically from phenols or quinones functional groups, is present in both WSB samples. In WSB7, it is at a slightly higher temperature and intensity compared to WSB5, as stated before, this suggests the presence of more stable oxygen functional groups, which decompose at higher temperatures. PIB biochar samples do not present peaks in this range; nonetheless, there is an increase in intensity that reflects the release of gases from less stable oxygenated groups. However, it is not as pronounced, suggesting that the oxygen-containing groups in PIB biochars are less abundant or less thermally stable compared to those in WSB biochars, confirming that the chemical composition plays a crucial role in the thermal stability and types of oxygenated groups present on the biochar surface. Higher and wider peaks around 800–900 °C, typically considered high-temperature peaks, are attributed to CO desorption, and less volatile organic

a) b)

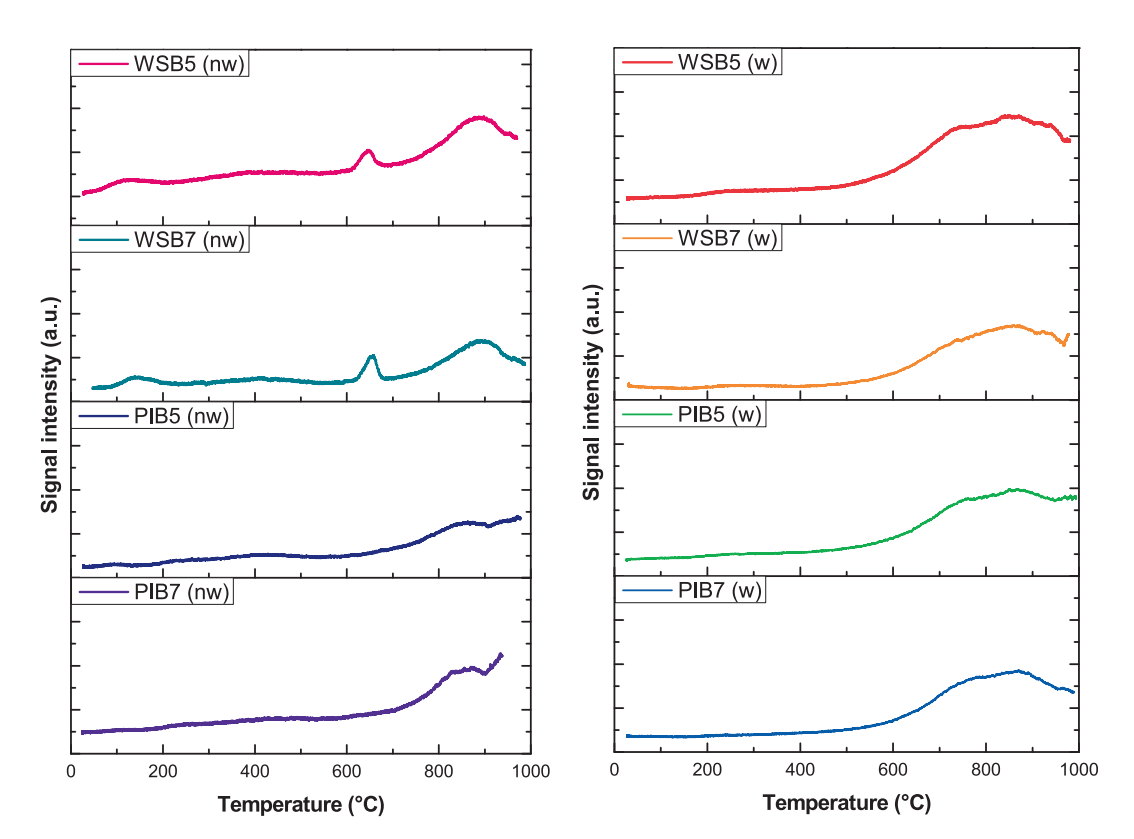


Fig. 2. He-TPD profiles of non-washed (section a) and acid-washed (section b) biochars.

compounds, highly stable aromatic carbon structures, or more stable oxygen-containing functionalities, such as carbonyl groups and quinones. WSB7 and WSB5 exhibit peaks around 900 °C, with WSB7 displaying a broader peak of relatively higher intensity, suggesting a more stable aromatic carbon structure or complex oxygenated compounds compared to WSB5. This difference indicates the impact of pyrolysis temperature on biochar surface functional groups. PIB biochars also present a signal in this range, but at slightly lower temperatures and intensity compared to WSB biochars. After the acid washing, TPD profiles are similar across all samples. The analyses show the effects on the thermal stability, indicating that the acid-washed activated biochar likely removed impurities and some labile and weaker oxygenated groups, leaving mostly stable oxygenated functional groups and aromatic structures, as previously highlighted in the FT-IR analyses. This is confirmed by the shift of the decomposition peaks to higher temperatures, enhancing the thermal stability of the remaining structure. Nonetheless, we can observe a gradual signal intensity increase around 700 °C and more pronounced at 800 °C, indicative of less stable oxygenated functional groups attributable to CO desorption. The TPD data clearly show that both pyrolysis temperature and biomass type significantly influence the thermal stability and surface chemistry of biochars. Higher pyrolysis temperatures result in more stable biochars with well-defined desorption peaks at higher temperatures, indicating the presence of stable aromatic and oxygenated structures. WS biochars show greater thermal stability than PS biochar, likely due to the differences in lignin content, which contributes to a more robust and complex carbon framework. In fact, the higher lignin content of WS, provides a more thermally stable carbon skeleton which is essential for withstanding the high-temperature activation process and facilitating the development of a robust microporous structure. The acid-wash

treatment effectively enhances the thermal stability of WS and PS biochars by removing labile oxygenated functional groups and impurities; it may also expose or alter the remaining functional groups, making them more prone to decomposition at the measured temperatures. This is evidenced by the shift of decomposition peaks to higher temperatures and the increased prominence, particularly in the WS biochars, which exhibit a more stable carbon structure post-wash. These components do not fully decompose at lower pyrolysis temperatures, leaving behind more reactive sites. The TPD curve of the commercial carbon (see supplementary materials, Fig. S2) shows a gradual increase in signal intensity as the temperature rises, with a peak around 800 °C, which suggests the release of stable oxygen-containing groups, likely carboxylic acids, lactones, or phenols. The high temperature required for the desorption indicates that these groups are relatively stable and strongly bound to the biochar's surface. From Table 3, reporting XPS results, it is evident that the washing process effectively eliminated excess oxygen

**Table 3**XPS composition of the main elements present on the surface of biochars.

Sample	C (%)	O (%)	Si (%)	Cl (%)	Na (%)	Ca (%)	Mn (%)	K (%)
WSB7 (nw)	95.8	3.9	-	0.3	-	-	-	-
WSB7 (w)	93	7	_	_	_	_	_	_
WSB5	97	3	_	-	-	_	-	_
(nw)								
WSB5 (w)	95.6	4	0.2	0.2	_	_	_	_
PIB7 (nw)	94.8	3.6	_	0.3	1	0.3	_	_
PIB7 (w)	97.3	2.5	_	0.2	_	_	_	_
PIB5 (nw)	73.4	14.0	_	2.6	6	_	1	3
PIB5 (w)	89.7	7.7	2.5	0.1	_	_	-	-

and reduced the level of contamination. This is illustrated by the absence of the K 2p doublet and the diminished relative intensity of the peak centered at 290 eV, which is associated with the formation of C-O bonds found in ester and carbonate chemical groups within the PIB5 sample post-washing (Fig. 3 and see supplementary materials, Fig. S3 and Fig.S4). The apparent discrepancy between elemental analysis and XPS results suggest an oxygen rich surface and a carbon- rich bulk..Th pH measurement since it provides insight into the acidity or alkalinity and is directly related to the functional groups present on the surface. Indeed, functional groups such as carboxylic, phenolic, hydroxylic, and amino groups are commonly found on the surface of biochars and depend on biomass characteristics or pyrolysis temperature. The pH determination is useful to predict how the biochar will interact with its environment, such as its potential to neutralize acidic or basic contaminants. At lower pH or in acidic conditions, the biochar is protonated or is another fundamental method for characterizing the surface chemistry of activated biochars has a positive charge; on the contrary, in basic conditions, the biochar's surface is negatively charged. The obtained pH values (Table 4) offer insights into how the washing step affects the chemical characteristics of the resulting biochars. Both WSB and PIB show a high pH value, around 10, typical of activated carbons. As expected, all samples show a significant drop in pH after acid washing, from strong alkaline (pH  $\sim 10$ ) to acidic (pH  $\sim 3$ –4). This is due to the removal of alkaline minerals (like carbonates) and the exposure of acidic surface functional groups, such as carboxyl, hydroxyls, and phenols. After washing, both WSB samples have slightly lower pH than PIB biochars, suggesting that acid washing has a more pronounced effect on removing basic components from WSB samples, leaving behind some acidic functionalities. This indicates a different mineral and organic composition of PIB compared to WSB, possibly with less basic content or more inherent acidic components. For example, PS contain a higher amount of calcium. Like the pH value, the PZC is a critical parameter in understanding biochar's surface chemistry, as it represents the pH at which the surface of the biochar carries no net charge. For instance, if the solution pH is above the pH<sub>pzc</sub>, the surface is likely to be negatively charged, enhancing the adsorption of cationic contaminants. Conversely, if the pH is below the  $pH_{\text{pzc}}$ , the surface may carry a positive charge, favoring anionic adsorption. pHpzc values (Table 4) are very similar across all samples, showing no drastic variation with pH<sub>pzc</sub> values around 7,9-8,4. This means that both biochars maintain a neutral to slightly basic pH at their pH<sub>pzc</sub> values, suggesting that pyrolysis temperature does not significantly affect the PZC values. pH<sub>pzc</sub> values are also very similar to the value of the commercial carbon, which is 8.2. The decrease in pH<sub>pzc</sub> values of all biochars after acid-wash treatment is consistent with the expected outcome of this step, which typically alters the surface characteristics of biochars by removing inorganic minerals and ash content.

Table 4 pH, pH $_{pzc}$ , and N $_2$  physisorption results (where S $_{BET}$ : BET surface area, S $_{LANG-MUIR}$ : Langmuir surface area, V $_{TOT}$ : total pore volume, V $_{micro}$ : total micropore volume, and V $_{meso}$ : total mesopore volume).

			•				
Sample	pН	$pH_{pzc}$	S <sub>BET</sub> (m <sup>2</sup> /g)	$S_{LANGMUIR}$ $(m^2/g)$	V <sub>TOT</sub> (cm <sup>3</sup> /g)	V <sub>micro</sub> (cm <sup>3</sup> / g)	V <sub>meso</sub> (cm <sup>3</sup> / g)
WSB7	10.1	8.2 $\pm$	545	$717 \pm 6$	0.3	0.2	0.1
(nw)	$\pm~0.1$	0.2	$\pm 6$				
WSB7	$3.5~\pm$	$6.7 \pm$	535	$719\pm7$	0.3	0.2	0.1
(w)	0.1	0.2	$\pm$ 5				
WSB5	10.2	8.2 $\pm$	608	$806 \pm 6$	0.3	0.2	0.1
(nw)	$\pm~0.1$	0.2	$\pm$ 7				
WSB5	3.4 $\pm$	6.8 $\pm$	570	$785 \pm 9$	0.3	0.2	0.1
(w)	0.1	0.2	$\pm$ 5				
PIB7	10.0	7.9 $\pm$	581	$784\pm10$	0.3	0.2	0.1
(nw)	$\pm~0.1$	0.2	$\pm$ 6				
PIB7	4.5 $\pm$	6.8 $\pm$	519	$701\pm7$	0.3	0.2	0.1
(w)	0.1	0.2	$\pm$ 5				
PIB5	10.0	8.4 $\pm$	557	$749\pm12$	0.3	0.2	0.1
(nw)	$\pm$ 0.1	0.2	$\pm 7$				
PIB5	4.7 $\pm$	7.1 $\pm$	593	$799\pm11$	0.3	0.2	0.1
(w)	0.1	0.2	$\pm$ 8				

Nitrogen physisorption analyses on the biochars (Fig. 4 and Table 4) were conducted to assess their surface properties, such as specific surface area, total pore volume, and pore size distribution. Adsorptiondesorption isotherms of non-washed PIB and WSB biochars (Fig. 4a) exhibit a similar sigmoidal shape, characteristic of both Type 1 and Type IV isotherms according to IUPAC classification. At low relative pressures (p/p $^{\circ}$  < 0.1), they show steep initial nitrogen adsorption that suggests the presence of micropores, characteristic of Type I isotherms. At p/p° higher than 0.4, the nitrogen adsorption increases continuously and exhibits a hysteresis loop, which indicates a significant presence of mesopores in each sample. The combination of these two features points to a mixed micro-mesoporous structure in the biochars, where both micropores and mesopores significantly contribute to the overall surface area and sorption capacity. WSB5 shows a relatively higher sorption capacity than WSB7, suggesting that WSB5 could retain more of its initial structure, allowing the development of mesopores, which may not be as pronounced for WSB7, even though higher pyrolysis temperatures usually promote greater carbonization, driving off more volatiles and resulting in a more developed porous carbon structure and enhancing microporosity. The slightly lower surface area of WSB7 compared to WSB5, can be attributed to the thermal stability of the walnut shell's lignin, which may have led to pore rearrangement or shrinkage rather than the expected increase in porosity. On the contrary, PIB5 shows a relatively lower sorption capacity than PIB7, which could suggest that this is due to the inherent composition of the biomasses, including a

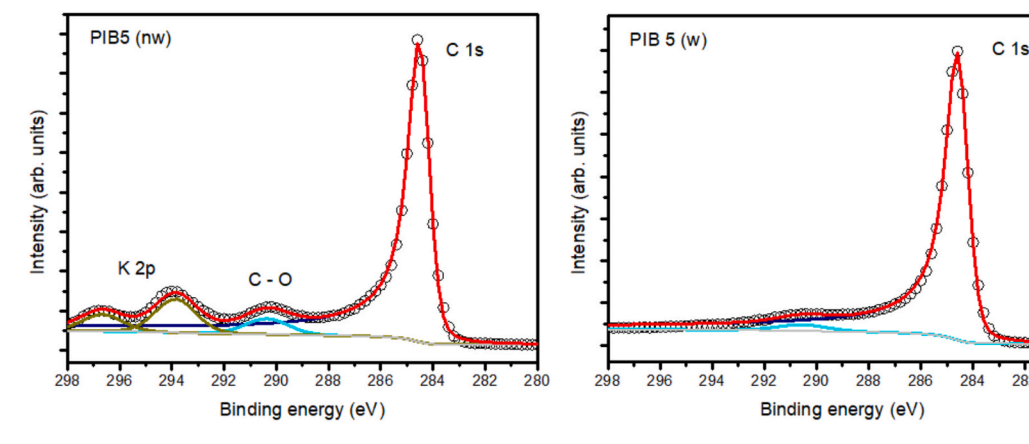


Fig. 3. The XPS spectra for the PIB5 sample were recorded both before and after acid washing. The spectrum obtained prior to washing indicates the presence of potassium, which is no longer detectable after the washing process.

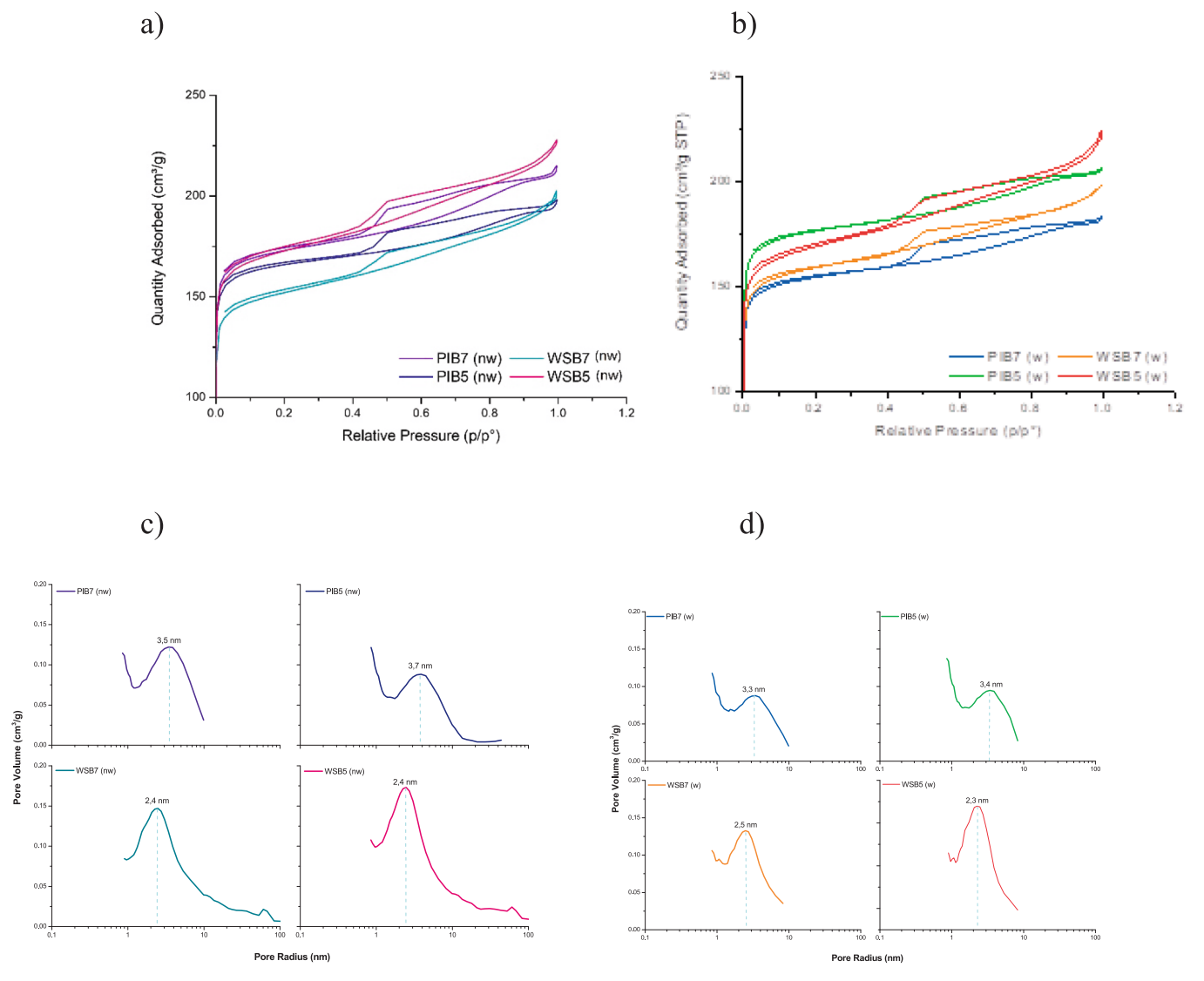


Fig. 4. Adsorption-desorption isotherms of non-washed (section a) and acid-washed (section b) biochars; Pore Size Distribution Curve of non-washed (section c) and acid-washed (section d).

different lignocellulosic structure that responds differently to pyrolysis temperature. PIB and WSB biochars exhibit a similar BET and Langmuir surface area of around  $500 - 600 \text{ m}^2/\text{g}$  and  $700-800 \text{ m}^2/\text{g}$ , respectively. Adsorption-desorption isotherms of WSB and PIB acid-washed samples still show (Fig. 4b) a hybrid isotherm between Type I and Type IV. However, washed samples pyrolyzed at 750 °C exhibit a relatively lower sorption capacity across the relative pressure range compared to their counterparts pyrolyzed at 500  $^{\circ}\text{C}\text{,}$  suggesting that a higher pyrolysis temperature (750 °C) in combination with acid-washing may favor the development of a pore structure more suitable for N2 sorption, particularly in mesoporous regions. WSB5 (washed) exhibited no significant change in sorption capacity, likely due to the retention of its initial structure after acid-washing, indicating that the treatment has a minimal impact on the superficial area and porosity. PIB7 (non-washed), as we saw before, showed a higher sorption capacity than PIB5 since the latter could retain more volatiles and inorganic matter due to lower pyrolysis temperature which can obstruct pores leading to a lower adsorption capacity, which is then increased after acid-washed this suggests the removal of more impurities, ash that could be decreasing pore accessibility and surface area. This improvement after acid-wash is less visible in the PIB7 sample since the acid-washing process can sometimes lead to the collapse or alteration of microporous structures,

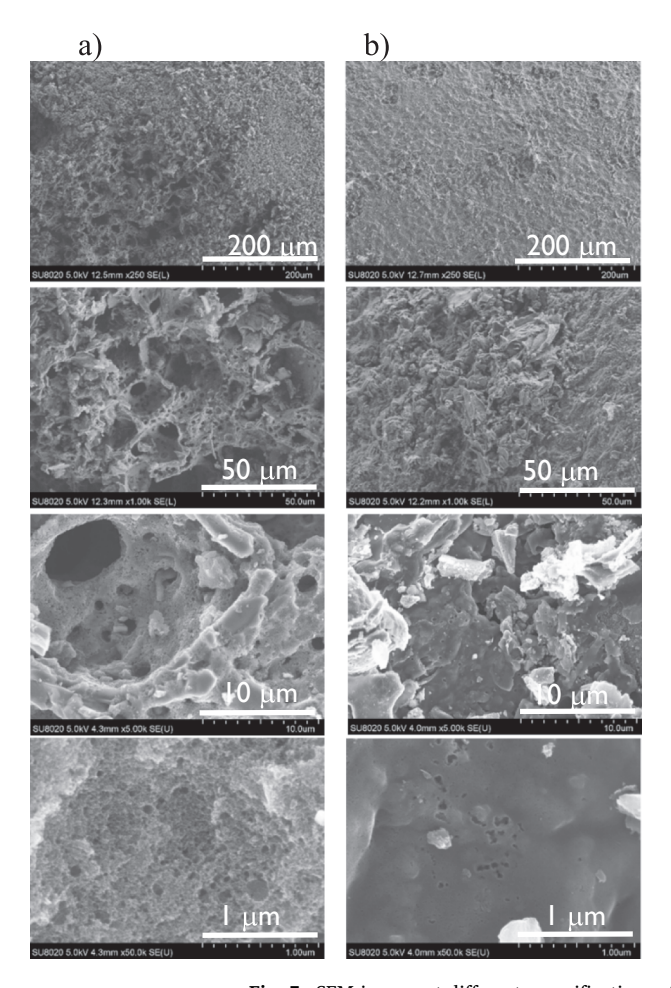
especially in highly carbonized biochars like PIB7 that may disrupt the delicate micropore structure, reducing the overall accessible surface area, also it could remove or damage the superficial carbon matrix, leading to a reduction in pore volume and surface area, which directly impacts adsorption capacity.

The higher pyrolysis temperature typically leads to greater microporosity and a higher surface area due to increased carbonization and removal of volatiles, which could suggest why PIB7 initially shows higher adsorption capacity than PIB5. Since acid-wash treatment is used to remove impurities that can block pores, this step could have a significant impact on higher-temperature pyrolyzed samples. Acid-wash treatment primarily influences the removal of surface impurities and minor or less stable structures on the surface, including functional groups, as analyzed with FT-IR and TPD results. Therefore, in both PIB and WBS biochar, BET and Langmuir show a slight change, suggesting that the acid-washing process has a relatively low impact on the overall surface area and surface structure. Total pore volume also presents minimal differences, suggesting similar pore structures and sorption potential. Commercial carbon shows the highest BET and Langmuir surface area (896 m<sup>2</sup>/g and 1286 m<sup>2</sup>/g, respectively), and total pore volume greater than PIB and WSB biochars (0.5 cm<sup>3</sup>/g, 0.2 cm<sup>3</sup>/g, 0.4 cm<sup>3</sup>/g). The effect of pyrolysis temperature on PIB and WSB biochars can impact the chemical composition, carbon stability, and pore accessibility formed at different temperatures. At lower temperatures, the carbonization process is less intense, resulting in a more amorphous structure with a higher proportion of volatile compounds and less thermal degradation of the biomass. This condition often leads to the formation of micropores as volatiles are gradually released. Higher energy input also tends to enhance the development of micropores as more volatiles are driven off, leaving behind a porous carbon skeleton. The result is typically a stable microporous structure with higher surface area and volume, as the high temperature facilitates the creation of clean, well-defined micropores. Nonetheless, pyrolysis conditions do not drastically impact the resulting surface area and pore volume.

PIB and WSB samples, regardless of the pyrolysis temperature and acid-washing, exhibit similar total micropore volumes of 0.2 cm<sup>3</sup>/g, suggesting that the acid-washing does not significantly affect the total micropore volume. However, acid-washing affects micropore and mesopore volumes differently depending on temperature, with lower temperatures showing more significant changes due to structural instability or unblocking effects. The curves display the pore size distribution curves obtained from BJH analysis for non-washed (Fig. 4, section c) and washed (Fig. 4, section d) samples. What was highlighted in the adsorption-desorption profiles is reflected in the pore distribution curves, which show a porous structure consistent with what has been previously discussed. The analyzed biochars (non washed and washed) all show a similar hysteresis loop attributable to a type IV profile. The adsorption branch is a composite of Types I and II, the more pronounced uptake at low p/p0 being associated with the filling of micropores. H4 loops are often found with aggregated crystals of zeolites, some mesoporous zeolites, and micro-mesoporous carbons as in this specific case.

Based on these results, the PIB and WSB biochars show promise for sorption applications, such as water treatment, air filtration, or soil remediation. Their comparable surface areas and stable pore volumes, combined with the minor variations in micropore volumes, indicate that both biochars are effective sorbents. Their inherent feedstock properties, including the pyrolysis temperature, are key factors in determining their suitability for different applications, suggesting that these biochars can be utilized effectively for a range of environmental and industrial processes.

From a morphological point of view, as highlighted by SEM micrographs (Fig. 5), some differences were observed between the PS and WS biochars, both before and after acid washing. All samples exhibited a fragmented and heterogeneous structure, which is consistent with previous studies (Phuong et al., 2015). The original structure is still partially visible, containing various types of pores, such as holes, pits, and cavities, resulting from the activation procedure, as demonstrated by the N<sub>2</sub> adsorption-desorption isotherms (Figs. 5a and c). WSB7(nw) displayed a sponge-like structure composed of deep cavities and holes with a diameter in the micron range (< 7 µm). In comparison, PIB7(nw) showed a similar corrugated structure with many defects but presented smaller pores ( $< 1 \mu m$ ). This sponge-like structure of the biochars is a key factor in adsorption as it can minimize the diffusive resistance for mass transport of the water on the biochar's surface. The SEM images also show that the biochar structure is largely preserved after acid washing for both samples (Figs. 5b and d). However, they did show a flatter morphology with some superficial macro-sized cavities and pores. This is likely due to the partial removal of impurities, as previously discussed in relation to the N2 physisorption results. Nevertheless, it can be assumed that most of the superficial pores are in the micro and meso



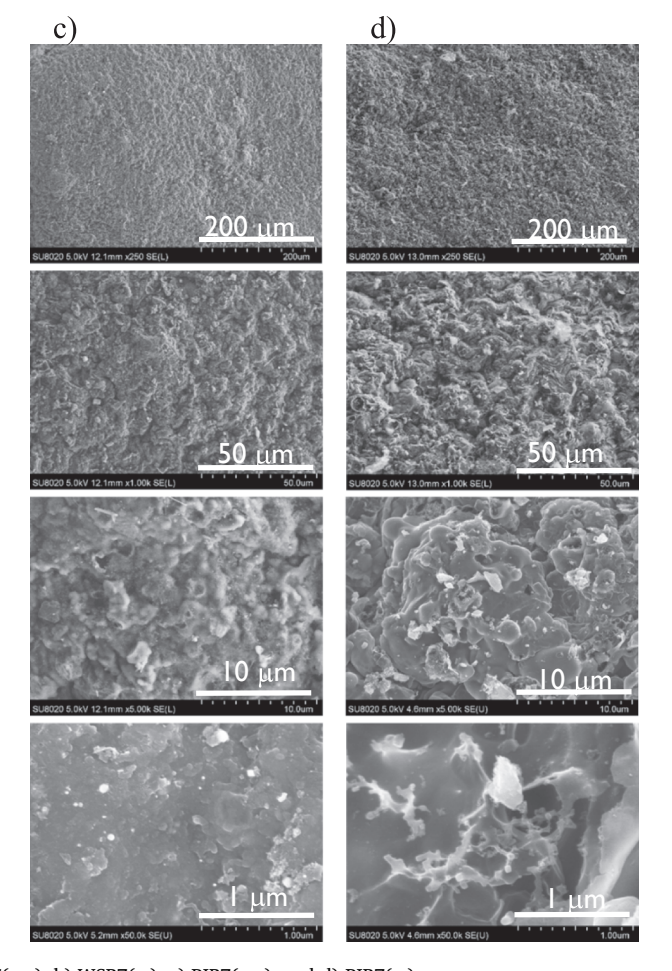


Fig. 5. SEM images at different magnifications of a) WSB7(nw), b) WSB7(w), c) PIB7(nw), and d) PIB7(w).

size range, as demonstrated by the  $N_2$  physisorption results, even though they are not visible in the SEM images due to the magnification limitations (Longo et al., 2023). Overall, despite differences in the shape and size of the pores, the biochars possess internal cavities, pores, and channels that contribute to their sorption properties.

The performances of the synthesized biochars were evaluated for the sorption of ATZ to determine their practical utility in water treatment (Fig. 6). Tests were conducted starting from 100 ppm of ATZ, which is under very stressed parameters. In fact, as mentioned in the introduction, the maximum allowable concentrations for drinking water typically range from 0.1 to 3  $\mu g/L$ . In contrast, the concentration in ground and surface water rarely exceeds the 2,0 ppm value and is commonly assessed around 0,1 ppm. Both PS and WS biochars exhibited high efficiencies after 10 cycles, achieving removal percentages in the range of 87-89 %. After 16 cycles, their performance improved, exhibiting a higher removal efficiency and achieving ATZ removal ranging from 94 to 95 %. Such values are similar to the performance of the commercial sample, which ranges from 97 % to 100 % of ATZ removal after 10 cycles. Calculated sorption capacities of biochars and commercial carbon are 0,18 mg/g. The effect of acid washing was found not to affect pesticide sorption, as the sorption of non-washed samples falls within the experimental error range, closely matching that of the corresponding washed activated biochars. The results showed the potential of both biochars to be a suitable option for removing ATZ and an alternative for longer-term performance applications due to their efficiency over time under such stressed conditions. PIB and WSB biochars present a high carbon content, which increased after being acid-washed. The delocalized  $\pi$ -electrons in the graphene layer are strongly correlated with the carbon content, which facilitates the  $\pi$ - $\pi$  interaction between biochar and the atrazine, due to its hydrophobic nature, increasing the adsorption capacity. The molecular properties of ATZ, a weak base with a pKa of 1.68, render it neutral at the pH of the experiments, thus minimizing the influence of the biochar's surface charge on its adsorption. This supports the conclusion that the high adsorption efficiency is driven by  $\pi$ - $\pi$  electron-donor-acceptor interactions between the ATZ and the graphitic surface of the biochar. Another important consideration is the presence of micropores in the biochars since the diameter of the ATZ molecule is 1 nm; hence, they can diffuse inside the micropores, with a diameter between 0,8 and 2 nm, which are the ones that regulate the sorption (Pelekani & Snoeyink, 2000). A qualitative analysis of this data suggests that the most important characteristic is the high surface area. In fact, samples with different characteristics in terms of functional groups, PZC or pH (ranging from 3.4 to 10.2) have a very similar sorption capacity. At the same time, commercial carbon, with its highest surface area, performs slightly better. To summarize, this study reports the production of activated biochars from agricultural waste, specifically walnut and pistachio shells. The process involved a two-step process: slow pyrolysis at 500 and 750 °C, followed by physical activation using CO<sub>2</sub> at 850 °C. This methodological approach effectively maximized the surface area and porosity of the biochars, thereby enhancing their sorption characteristics. These results highlight the significant potential of activated biochars as effective sorbents for herbicide remediation in wastewater treatment. The biochars demonstrated high adsorption capacities for ATZ, with performance comparable to that of commercial activated carbon. This is particularly relevant considering increasing regulatory pressures regarding the environmental impacts of synthetic herbicides and the need for sustainable, cost-effective remediation strategies. The effect of acid washing was found not to affect pesticide adsorption, unlike metal adsorption (Harabi, et. al, 2024; Chen, J.P. & Wu, S., 2004). Furthermore, WS possess a dense and robust structure that contributes to the formation of biochar with high mechanical strength, advantageous for applications requiring repeated use or where the biochar must endure physical stress, and limit the risk of leaching. Future research should focus on scaling up the production of biochars and assessing their long-term performance in real-world wastewater treatment scenarios. Additionally, investigations

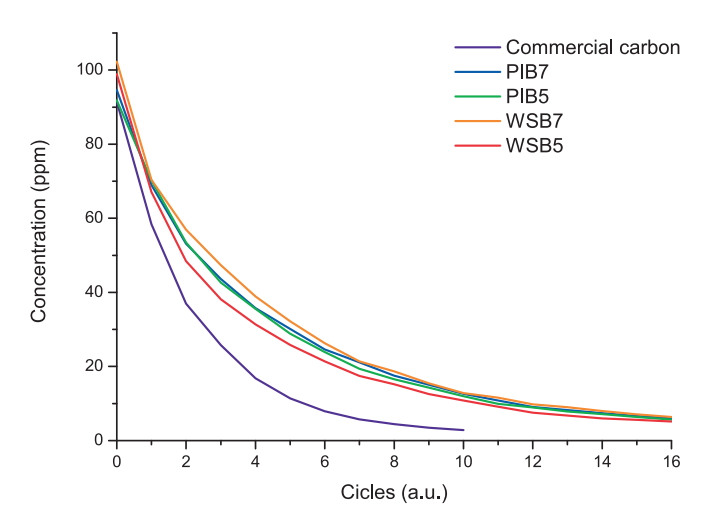


Fig. 6. Variation of the concentration of atrazine in the aqueous solution of washed biochars.

into the regeneration and reusability of these biochars could further enhance their feasibility as a sustainable solution for herbicide contamination. By converting abundant agricultural residues into high-value sorbents, this approach addresses pollution while contributing to sustainable agricultural practices.

#### 4. Conclusions

This study evaluated the efficiency of activated biochars from agricultural waste, specifically walnut and pistachio shells, in removing the herbicide atrazine from contaminated water. These biochars, thanks to their surface area and dense network of small pores, could be effective at sorbing also other organic molecules with a suitable size, such as other pesticides and herbicides, pharmaceuticals and personal care products, industrial and aromatic pollutants, organic dyes. Surface area appears to be the most important parameter for sorption performance. The research aligns with the principles of the circular economy, promoting waste valorization and resource efficiency. Overall, the findings provide a compelling case for the adoption of activated biochars in the ongoing efforts to mitigate the environmental impacts of agricultural chemicals.

## **Ethical approval**

This article does not contain any studies with human participants or animals performed by any of the authors.

## CRediT authorship contribution statement

Federica Menegazzo: Writing – review & editing, Writing – original draft, Validation, Conceptualization. Rony Snyders: Supervision. Carla Bittencourt: Writing – review & editing, Formal analysis. Melissa Del Carmen Bello Pinzon: Formal analysis. Elena Ghedini: Methodology, Data curation. Michela Signoretto: Supervision, Resources.

## Declaration of competing interest

The authors declare that they have no known competing financial interests or personal relationships that could have appeared to influence the work reported in this paper.

## Acknowledgment

FM thanks the "Fonds de la Recherche Scientifique- F.R.S.-FNRS" for the "Bourse de Sejour scientifique" (2025/V6/5/015-JG/DeM-604) that made possible this scientific collaboration. Mrs. Tania Fantinel is kindly acknowledged for technical assistance.

#### Appendix A. Supplementary data

Supplementary data to this article can be found online at https://doi.org/10.1016/j.biortech.2025.133367.

## Data availability

The authors declare that the data supporting the findings of this study are available within the paper. Other eventual supplementary information is available from the authors on reasonable request.

#### References

- Apolloni, F., Menegazzo, F., Bittencourt, C., Signoretto, M., 2025. Hazelnut shells and rice husks activated biochars for the adsorption of atrazine and terbuthylazine. Next Energy 7, 100291
- Čolnik, M., Irgolič, M., Perva, A., Škerget, M., 2024. The Conversion of Pistachio and Walnut Shell Waste into Valuable Components with Subcritical Water. Processes 12 (1), 195.
- Deng, S., Chen, C., Wang, Y., Liu, S., Zhao, J., Cao, B., Zhang, Y., 2024. Advances in understanding and mitigating Atrazine's environmental and health impact: a comprehensive review. J. Environ. Manag. 365, 121530.
- Dong, X., Chu, Y., Tong, Z., Sun, M., Meng, D., Yi, X., Duan, J., 2024. Mechanisms of adsorption and functionalization of biochar for pesticides: a review. Eco. Environ. 272, 116019.
- Fordos, S., Abid, N., Gulzar, M., Pasha, I., Oz, F., Shahid, A., Aadil, R., 2023. Recent development in the application of walnut processing by-products (walnut shell and walnut husk). Biomass Convers. Biorefin. 13, 14389–14411.
- Fu, P., Hu, S., Xiang, J., Li, P., Huang, D., Jiang, L., Zhang, A., Zhang, J., 2010. FTIR Study of Pyrolysis Products Evolving from typical Agricultural Residues. J. Anal. Appl. Pyrol. 88, 117–123.
- Gao, B., Wang, Y., Huang, L., Liu, S., 2021. Study on the performance of HNO3-modified biochar for enhanced medium temperature anaerobic digestion of food waste. Waste Manag. 135, 338–346.
- Gatabi, M., Milani Moghaddam, H., Ghorbani, M., 2015. Point of zero charge of maghemite decorated multiwalled carbon nanotubes fabricated by chemical precipitation method. J. Mol. Liq. 216, 117–125.
- Halysh, V., Sevastyanova, O., Riazanova, A., Pasalskiy, B., Budnyak, T., Lindström, M., Kartel, M., 2018. Walnut shells as a potential low-cost lignocellulosic sorbent for dyes and metal ions. Cellul. 25 (8), 4729–4742.
- Handiso, B., Pääkkönen, T., Wilson, B., 2024. Effect of pyrolysis temperature on the physical and chemical characteristics of pine wood biochar. Waste Manag. Bull. 2 (4) 201-207
- Hosseinzaei, B., Hadianfard, M., Aghabarari, B., García-Rollán, M., Ruiz-Rosas, R., Rosas, J., Cordero, T., 2022. Pyrolysis of pistachio shell, orange peel and saffron petals for bioenergy production. Bioresour. Technol. Rep. 19, 101209.
- Hu, C., Zhang, J., Chen, Y., Zhang, W., Ji, R., Song, Y., Han, J., 2022. Hierarchical porous biochars with controlled pore structures derived from co-pyrolysis of potassium/ calcium carbonate with cotton straw for efficient sorption of diethyl phthalate from aqueous solution. Bioresour. Technol. 346, 126604.
- Huang, W.-H., Lee, D.-J., Huang, C., 2021. Modification on biochars for applications: a research update. Bioresour. Technol. 319, 124100.
- Janu, R., Mrlik, V., Ribitsch, D., Hofman, J., Sedláček, P., Bielská, L., Soja, G., 2021. Biochar surface functional groups as affected by biomass feedstock, biochar composition and pyrolysis temperature. Carbon Res. Convers. 4, 36–46.
- Khoshnood, Z., 2024. A review on toxic effects of pesticides in Zebrafish, Danio rerio and common carp, Cyprinus carpio, emphasising Atrazine herbicide. Toxicol. Rep. 13, 101694
- Kim, Y., Oh, J.-I., Vithanage, M., Park, Y.-K., Lee, J., Kwon, E., 2019. Modification of biochar properties using CO2. Chem. Eng. J. 372, 383–389.
- Kokab, T., Ashraf, H., Shakoor, M., Jilani, A., Ahmad, S., Majid, M., Bahar, M., 2021.
  Effective Removal of Cr(VI) from Wastewater using Biochar Derived from Walnut Shell. Int. J. Environ. Res. Public Health 18, 9670.

- Korkut, A., 2011. Thermogravimetric analysis of walnut shell as pyrolysis feedstock. J. Therm. Anal. Calorim. 105 (1), 145–150.
- Longo, L., Taghavi, S., Ghedini, E., Menegazzo, F., Di Michele, A., Cruciani, G., Signoretto, M., 2022. Selective hydrogenation of HMF to 1-hydroxy-2,5-hexanedione by biochar supported Ru catalysts. ChemSusChem 15 (13).
- Longo, L., Taghavi, S., Riello, M., Ghedini, E., Menegazzo, F., Di Michele, A., Cruciani, G., Signoretto, M., 2023. Waste biomasses as precursors of catalytic supports in benzaldehyde hydrogenation. Catal. Today 420, 114038.
- Lu, X., Gu, X., 2022. A review on lignin pyrolysis: pyrolytic behavior, mechanism, and relevant upgrading for improving process efficiency. Biotechnol. Biofuels Bioprod. 15 (1), 106.
- Muzyka, R., Misztal, E., Hrabak, J., Banks, S., Sajdak, M., 2023. Various biomass pyrolysis conditions influence the porosity and pore size distribution of biochar. Energy 263, 126128.
- Nair, R., Schaate, A., Klepzig, L., Turcios, A., Lecinski, J., Shamsuyeva, M., Weichgrebe, D., 2023. Physico-chemical characterization of walnut shell biochar from uncontrolled pyrolysis in a garden oven and surface modification by ex-situ chemical magnetization. Clean Techn. Environ. Policy 25 (8), 2727–2746.
- Ozpinar, P., Dogan, P., Demiral, C., Morali, H., Erol, U., Samdan, S., Yildiz, D., Demiral, I., 2022. Activated Carbons Prepared from Hazelnut Shell Waste by Phosphoric Acid Activation for Supercapacitor Electrode applications and Comprehensive Electrochemical Analysis. Renew. Energy 189, 535–548.
- Pączkowski, P., Gawdzik, B., 2024. Synthesis, characterization and degradation studies of eco-friendly composites from thermoset resins with pistachio shell waste. J. Therm. Anal. Calorim. 149 (7), 2789–2804.
- Pelekani, C., Snoeyink, V.L., 2000. Competitive adsorption between atrazine and methylene blue on activated carbon: the importance of pore size distribution. Carbon 38, 1423–1436.
- Phuong, H.T., Uddin, M.A., Kato, Y., 2015. Characterization of biochar from pyrolysis of rice husk and rice straw. J. Biobaased Mater. Bioenergy 9, 439–446.
- Rambhatla, N., Florence Panicker, T., Kumar Mishra, R., Kini Manjeshwar, S., Sharma, A., 2025. Biomass pyrolysis for biochar production: Study of kinetics parameters and effect of temperature on biochar yield and its physicochemical properties. Results Eng. 25, 103679.
- Saracoglu, M., Coruh, M., 2024. Thermal degradation properties, kinetic, thermodynamic and reaction mechanism of pyrolysis of biomass shells: pistachio, almond, walnut and hazelnut as bioenergy potential. Biomass Convers. Biorefin. 14, 32427–32452.
- Singh, J., Verma, M., 2024. Waste derived modified biochar as promising functional material for enhanced water remediation potential. Environ. Res. 117999.
- Singh, S., Kumar, V., Chauhan, A., Datta, S., Wani, A., Singh, N., Singh, J., 2018. Toxicity, degradation and analysis of the herbicide atrazine. Environ. Chem. Lett. 16 (1), 211–237.
- Song, Y., Jia, Z., Chen, J., Hu, J., Zhang, L., 2014. Toxic Effects of Atrazine on Reproductive System of Male Rats. Biomed. Environ. Sci. 27 (4), 281–288.
- Tan, X., Liu, Y., Zeng, G., Wang, X., Hu, X., Gu, Y., Yang, Z., 2015. Application of biochar for the removal of pollutants from aqueous solutions. Chemosphere 125, 70–85.
- Tillvitz do Nascimento, C., Gurgel Adeodato Vieira, M., Bisinella Scheufele, F., Palú, F., da Silva, E., Borba, C., 2022. Adsorption of atrazine from aqueous systems on chemically activated biochar produced from corn straw. J. Environ. Chem. Eng. 10 (1), 107039.
- Uba Zango, Z., Garba, A., Haruna, A., Shehu Imam, S., Usman Katsina, A., Fate Ali, A., Adamu, H., 2024. A systematic review on applications of biochar and activated carbon derived from biomass as sorbents for sustainable remediation of antibiotics from pharmaceutical wastewater. J. Water Process Eng. 67, 106186.
- Wang, S., Dai, G., Yang, H., Luo, Z., 2017. Lignocellulosic biomass pyrolysis mechanism: a state-of-the-art review. Prog. Energy Combust. Sci. 33–86.
- Wang, X., Guo, Z., Hu, Z., Zhang, J., 2020. Recent advances in biochar application for water and wastewater treatment: a review. PeerJ: Environ. Sci. https://doi.org/ 10.7717/peerj.9164.
- Zhang, P., Duan, W., Peng, H., Pan, B., Xing, B., 2022. Functional Biochar and its Balanced Design. ACS Environ 2 (2), 115–127.
- Zhi, F., Zhou, W., Chen, J., Meng, Y., Hou, X., Qu, J., Hu, Q., 2023. Adsorption properties of active biochar: Overlooked role of the structure of biomass. Bioresour. Technol. 387, 129695.